



Moisture changes and fluctuations of the Westerlies in Mediterranean Central Chile during the last 2000 years: The Laguna Aculeo record (33°50'S)

Bettina Jenny^{a,*}, Blas L. Valero-Garcés^b, Roberto Urrutia^c, Kerry Kelts^{d,1}, Heinz Veit^a, Peter G. Appleby^e, Mebus Geyh^f

^a Department of Physical Geography, University of Bern, Hallerstrasse 12, 3012 Bern, Switzerland

^b Pyrenean Institute of Ecology, Spanish Scientific Research Council, Apdo 202, Zaragoza 50080, Spain

^c Centro EULA-Chile, University of Concepción, Casilla 160-C, Concepción, Chile

^d Limnological Research Center, 220 Pillsbury Hall, University of Minnesota, Minneapolis, MI 55455, USA

^e Environmental Radioactivity Research Centre, University of Liverpool, P.O. Box 147, Liverpool L69 3BX, UK

^f Institute for Joint Geoscientific Research, Stilleweg 2, Hannover 30655, Germany

Abstract

The multi-proxy study of lacustrine sediments from Laguna Aculeo (33°50'S) provides detailed information about moisture changes in the lowlands of Mediterranean Central Chile during the last 2000 years. The lake lies just at the northern border of the strong Westerlies influence with dry summers and humid winters. Geochemical, sedimentological and diatom analyses provide evidence for an arid period between cal 200 BC and AD 200 and a subsequent increase in moisture after cal AD 200. Abundant clastic layers in the core represent flood events. Periods with a higher frequency of flood events indicate an increased intensity of the Westerlies, more winter frontal system activity and possibly ENSO-related variability, probably comparable to modern conditions in Mediterranean Central Chile. Periods of high clastic input occur around cal AD 200–400, 500–700, especially around cal AD 1300–1700, and around AD 1850–1998. During the last 50 years, at least eight flood events were detected, correlating mainly with El Niño years. A very short drier period also occurred in the late 1960s. In recent decades, human impact has resulted in a eutrophication of the lake. © 2001 Elsevier Science Ltd and INQUA. All rights reserved.

1. Introduction

The area around 34°S in Mediterranean Central Chile is situated at the northern border of the strong influence of the Westerly circulation belt (Westerlies). The gradient of precipitation is especially steep in that region with a high moisture supply in the south and increasingly drier conditions towards the north. Consequently, palaeoclimate archives in Central Chile are expected to have been very sensitive to past humidity changes related to fluctuations of the Westerlies in southern South America. Knowledge of Holocene climatic change in Central Chile, however, is still sparse (e.g. Heusser, 1983, 1990; Villa-Martínez and Villagrán,

1997; Lamy et al., 1999). Consensus exists about the occurrence of a mid-Holocene arid phase and the onset of more humid conditions about 3000 ¹⁴C yr BP (e.g. Markgraf, 1989; Villagrán and Varela, 1990; Veit, 1996). In order to explain mid-Holocene aridity in Mediterranean Chile, Markgraf (1989) suggests a stronger influence of the Southeast Pacific high-pressure cell blocking the Westerly frontal system. Further north, on the Chilean Altiplano, however, the palaeoclimate archives are more sensitive to moisture changes related to the tropical circulation (e.g. Valero-Garcés et al., 1996; Grosjean et al., 1997).

In the lowlands of Mediterranean Central Chile, there are few natural lakes due to the semiarid climate. The Tagua Tagua pollen profile (34°30'S) investigated by Heusser (1983, 1990) provides reconstructions of the vegetational history since the late Pleistocene. However, due to the drainage of the lake for agricultural use, the late Holocene is not well preserved. Pollen data from Quintero (32°47'S, 71°29'W), a swamp site at the

*Corresponding author.

E-mail address: jenny@giub.unibe.ch (B. Jenny).

¹ The authors dedicate this paper to Kerry Kelts, a great scientist and friend, whose global thinking and passion for lakes were extremely inspiring. He passed away on February 8, 2001.

Chilean coast, suggest increasingly wet conditions starting around 4000 ^{14}C yr BP, and the establishment of present-day forest and a more humid climate around 2000 ^{14}C yr BP (Villa-Martínez and Villagrán, 1997). Detailed tree ring studies in Central Chile and Northern Patagonia from the last millennium (e.g. Villalba, 1994a, b; Boninsegna, 1990) generally indicate a cold-moist period between cal AD 1270 and 1670. In the Norte Chico (around 30°S), Veit (1996), based on paleosol studies, also identifies two humid periods around cal AD 0–400 and 1300–1800, and he interprets increased moisture as a result of intensified Westerlies.

The present paper provides the first detailed multiproxy lake study of the late Holocene in Mediterranean Central Chile. Sedimentological, geochemical and diatom analyses as well as age control, based on ^{210}Pb , AMS and conventional ^{14}C dates, allow a detailed climatic reconstruction of the last 2000 years. The accurate and reliable chronological framework allows detection of decadal to centennial changes in the intensity of the Westerlies in South America.

2. Geographical and geological conditions

The Laguna Aculeo (33°50'S, 70°54'W, 350 m a.s.l.) is situated 50 km southeast of the capital, Santiago de Chile. With a surface of 12 km² and a depth of up to 6 m, it is one of the largest natural lakes in the region. The lake lies in a tectonic basin in the Coastal Cordillera of Central Chile (Fig. 1). The bedrock in the catchment area consists mainly of Cretaceous and Tertiary andesites. The basin is bounded to the south by a Cretaceous intrusion of granodiorites and tonalites (Corvalán and Munizaga, 1972). Outcrops of sedimentary rocks are very much restricted and carbonate rocks are absent in the catchment. The lake is surrounded by Quaternary alluvial fan deposits originating from the coastal Cordillera, and particularly well developed on the eastern side of the basin. Mountains higher than 2000 m surround the lake. There is no direct inflow from the Andes. Laguna Aculeo shows a high sensibility to heavy storm events, because of the steep relief around the lake, and the presence of ephemeral creeks, which are able to transport water and sediments quickly into the lake. The lake has a small outflow on the eastern side, which runs dry in summer, is rarely filled with water even in winter, and at times in rainy winters even functions as an inflow (Cabrera and Montecino, 1982). As this very small outflow can be virtually neglected, the system behaves almost like a closed basin (Vila, pers. comm., 1998). Hence, evaporation is the main process of water loss. Table 1 gives the modern conditions of the lake water. The lake became a tourist attraction in the 1960s. Current land use is mainly related to agriculture

and tourism. Today, the lake is a highly eutrophic system (Cabrera and Montecino, 1982).

3. Climate

The climate in the lowlands of Central Chile is Mediterranean. The summer is dry with high radiation and evaporation rates because the very stable subtropical high-pressure cell blocks the frontal system of the Westerlies. The winter is cooler and humid, with positive moisture balance, as the Westerlies reach Central Chile (Weischet, 1996).

The seasonality of precipitation changes most rapidly around 34°S. South of 34°S, winter precipitation is dominant and regular, while north of 34°S, winter precipitation occurs episodically (Van Husen, 1967). Laguna Aculeo (33°50'S) lies at the border of the strong Westerly influence. Hence, palaeoclimate archives at this site should record changes in moisture supply and in the intensity of the Westerlies. Average annual precipitation in the last 50 years is 545 mm, but more than 1000 mm/yr is common in El Niño years (Fig. 2a). Potential evaporation exceeds precipitation in general. The mean temperature in Central Chile is around 8–10°C in winter and 18–20°C in summer (Weischet, 1996, Fig. 2b).

In Central Chile, high annual precipitation is correlated with El Niño years at least during the last 50 years (Fig. 2a). In the lowlands of Central Chile, all years showing high precipitation correspond to El Niño years, while not all El Niño years correspond to high annual precipitation. Aceituno (1989) shows that during El Niño years, the temperature gradient between the tropics and the higher latitudes increases and therefore the Westerly activity is generally stronger with more frontal activity and rainfall.

4. Methods

Two sediment cores, 172 and 100 cm long (for ^{210}Pb analyses), were taken from the deepest part of Laguna Aculeo in 1998 using a modified Livingston piston corer of 5 cm diameter (Fig. 1). The 172 cm core was split into half and photographed. The facies and sedimentary units were determined using lithology, organic macrorests, sedimentary structures, smear slides and thin sections. Whole-core magnetic susceptibility was measured in the field prior to subsampling of the 100 cm core for ^{210}Pb dating. Magnetic susceptibility with a Bartington susceptibility bridge and wet density were determined in the laboratory at 0.5 cm intervals in the 172 cm core.

Subsamples were taken for every cm and freeze-dried. Carbon content was measured with a CM5012 CO₂ coulometer. Organic carbon content was determined as

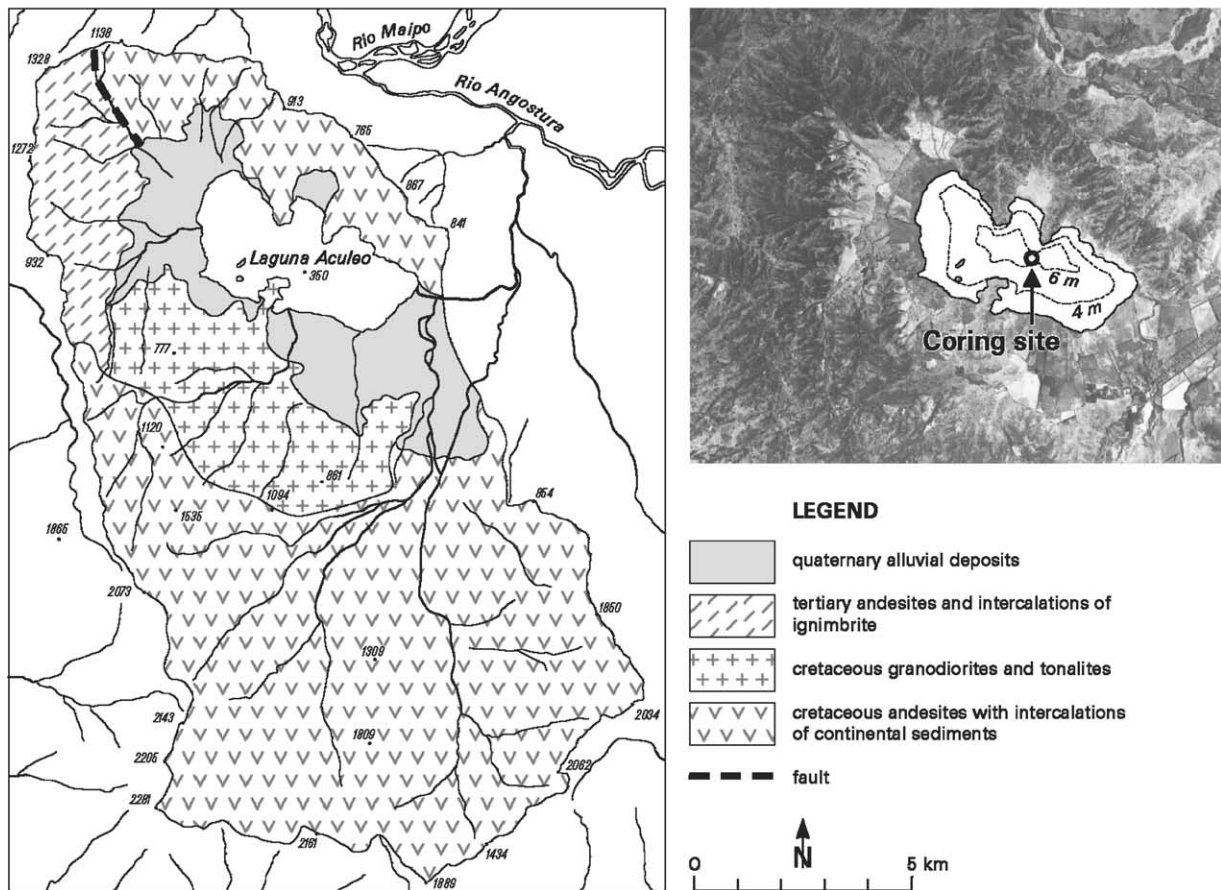
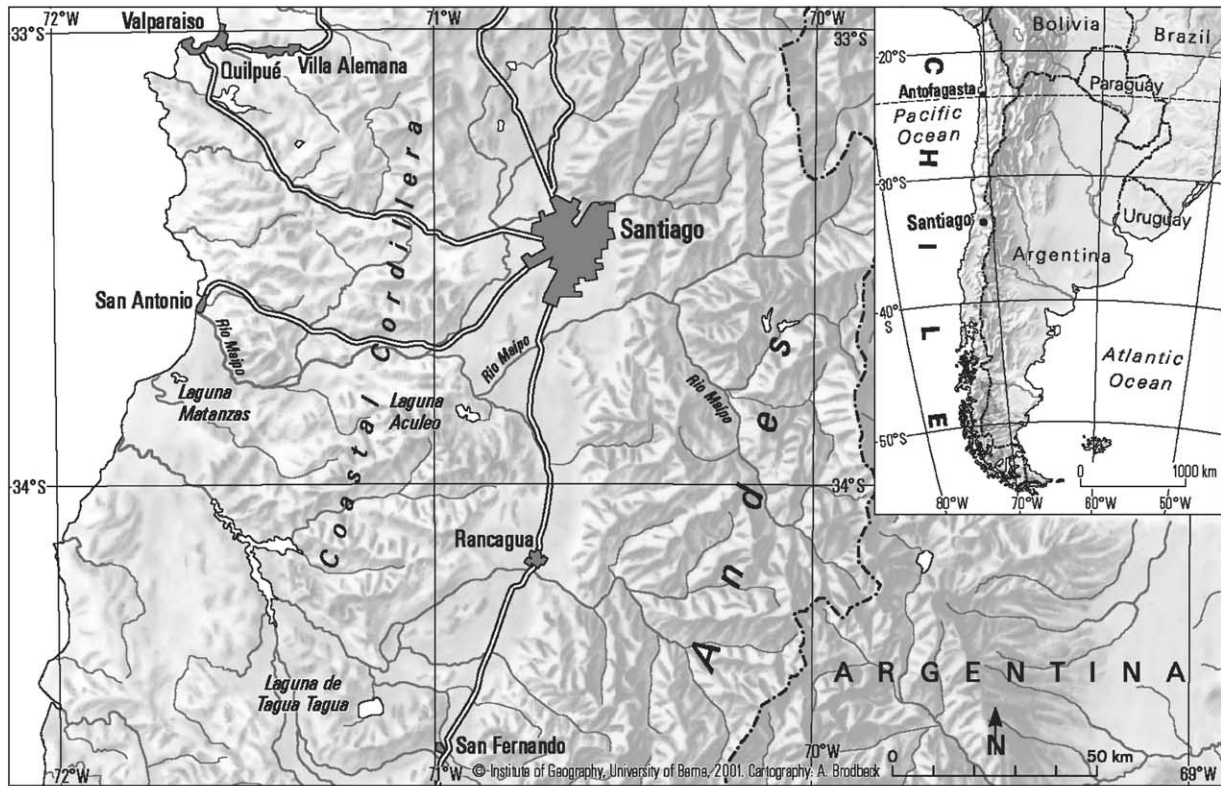


Fig. 1. Overview of the geographic and geologic setting of Laguna Aculeo and location of the coring site. Geologic units are indicated according to Corvalán and Munizaga (1972). Due to the very steep catchment, many creeks enter the lake and are only sporadically filled with water in rainy winters. The southeastern part of the catchment does hardly drain into the lake but into the river Maipo.

total carbon content minus the inorganic carbon content. There was neither dolomite nor siderite in the samples. Therefore, the amount of CaCO_3 was directly calculated from inorganic carbon. For the determination of major cations and trace metals, 50 mg subsamples were digested in 3 M HNO_3 and agitated for 12 h, then measured on a Liberty ISOAX Varian ICP. Samples for water-soluble anion measurements were agitated in pure water for 24 h, centrifuged, filtered and determined by ion chromatography (Dionex-120).

Approximately 0.1 g of dry sediment was processed for diatom analyses using sulfuric acid, potassium permanganate and oxalic acid (Hasle and Fryxell,

1970). Material was dried onto coverslips and mounted in Hyrax ($n = 1.7$) mounting medium. Diatoms were identified under a Carl Zeiss Axioplan microscope with an oil immersion objective magnified $1000\times$. A minimum of 500 frustules were counted in random transects (relative abundance). Diatoms were classified based on Rivera et al. (1982) and Krammer and Lange-Bertalot (1988, 1991a, b). Autoecological characteristics of the most important species with respect to total phosphorus (TP), salinity, life form and trophic state were mainly obtained from Schoemann (1973), Van Dam et al. (1994), Cumming et al. (1995) and Dixit et al. (1999). Biogenic silica was calculated after the method of Mortlock and Froelich (1989), a wet-alkaline extraction procedure.

In order to date the uppermost sediments between 0 and 50 cm, samples were analyzed for ^{210}Pb and ^{137}Cs by direct gamma assay using Ortec HPGe GWL series well-type coaxial low background intrinsic germanium detectors (Appleby et al., 1986). Below 50 cm, organic material samples were dated by AMS and conventional ^{14}C techniques.

Table 1

Chemical composition of the water of the Laguna Aculeo and of the groundwater (8 February 1998, noon)

| Parameter | Lake water | N side (ground-water) (33°50.5'S, 70°54.4'W) | SE side (inflow about 31/s) (33°52.4'S, 70°54.2'W) | W side (ground-water) (33°49.35'S, 70°56.5'W) |
|-------------------------|------------|--|--|---|
| Temperature °C | 27.9 | — | 21.1 | 28.9 |
| El. cond. (uS/cm) | 244 | 1050 | 421 | 150 |
| pH | 7 | 6.0 | 6.5 | 5.5 |
| Salinity (%) | 0 | 0.3 | 0 | 0 |
| Ca (µg/ml) | 17.1 | 14.1 | 29.7 | 12.8 |
| Mg (µg/ml) | 8.63 | 5.75 | 13.9 | 2.95 |
| K (µg/ml) | 3.03 | 0.67 | 2.32 | 1.0 |
| Sr (µg/ml) | 0.137 | 0.093 | 0.246 | 0.0688 |
| Na (µg/ml) | 19.4 | 10.5 | 29.6 | 10.7 |
| Cl (µg/ml) | 6.01 | — | — | — |
| SO ₄ (µg/ml) | 16.16 | — | — | — |

5. Results

In the following sections, we describe the results and also the interpretation of the environmental information provided by the different proxies in more detail. Based on all available data, four sedimentary units were defined in the core: unit 1: 0–66 cm; unit 2: 66–122 cm; unit 3: 122–163 cm and unit 4: 163–172 cm.

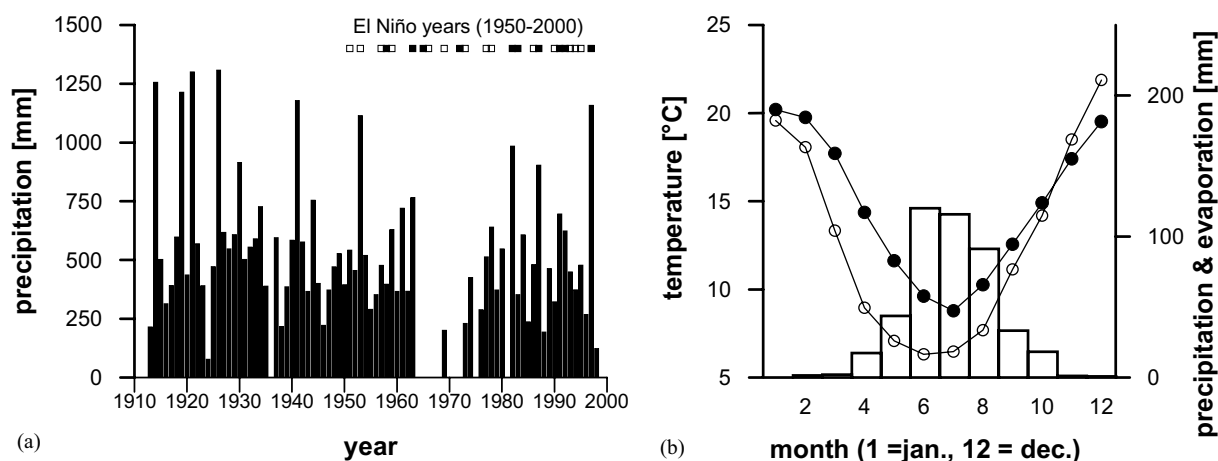


Fig. 2. (a) Overview of the annual precipitation at Laguna Aculeo during the 20th century. Average annual rainfall is 545 mm, but easily exceeds 1000 mm, mainly during El Niño years. Open dots: weak El Niño years and solid dots: normal and strong El Niño years. There is a lack of precipitation data for the years 1936, 1964–1968, 1969–1972, 1975 and 1981. (Precipitation data adapted from Dirección General de Aguas, Chile; El Niño data adapted from the Climate prediction center, NOAA, USA); (b) monthly distribution of precipitation, evaporation and temperature at Laguna Aculeo. Open dots: evaporation; solid dots: temperature and bar graph: precipitation. Data are based on the years 1989–1991 and 1994–1998. There is a high seasonality of the precipitation with rainy winters and dry summers. Evaporation and temperature show a similar pattern, with low values in winter. In summer, however, potential evaporation exceeds precipitation. (Data adapted from Dirección General de Aguas, Chile).

5.1. Sedimentology

The Laguna Aculeo sediment core is composed of greenish, massive to banded, organic-rich sediments with numerous intercalated, centimeter-thick grey, fine-grained clastic layers. Sediments are composed of lacustrine organic matter, biogenic particles (diatoms, ostracods), silicate grains, and carbonates. Carbonate content in the core sediments is practically zero, except for two intervals with significant values (around 10%) at 163–172 and 30–40 cm. Organic carbon values are high, ranging between 5% and 30%. There are three major intervals with high organic matter content around 163–172 cm, 120–150 cm, and in the uppermost 25 cm. Organic carbon content in the fine-grained clastic grey layers is 0%. Based on sediment composition and sedimentological textures and structures, three main sedimentary facies were identified (Fig. 3).

Facies 1: Dark greenish, massive to banded, organic-rich, diatomaceous sediments. They occur as cm- to dm-thick layers, commonly massive and with non-erosive lower contacts. The sediments are mostly composed of lacustrine (algae and macrophytes) organic matter (up to 25% TOC) and biogenic material (diatoms). Diatom content is high as determined by microscope estimates and biogenic silica (up to 20%). Carbonate is practically absent (<1%).

Facies 2: Light greenish, banded to laminated, diatomaceous sediments with abundant plant remains. They occur as cm-thick layers, frequently with erosive upper and lower contacts. Facies 2 shows organic matter content similar to that of Facies 1, although the percentage of macrophyte remains is higher in Facies 2. Some terrestrial plant remains also occur. Diatom content is lower than in Facies 1. Silicate components (quartz, micas, feldspar) are also present and may reach significant percentages in some layers. Mm-long grey, silty intraclasts are common. Carbonate content is significant, and reaches 10% in some cases (163–172 and 30–40 cm intervals). Ostracods are only present in the lower interval (163–172 cm).

Facies 3: Grey, massive to laminated, silty clays. Facies 3 occurs as cm-thick, massive to laminated layers with sharp and erosive lower contacts. More than 20 clastic layers appear, many of them showing fining-upward textures. These layers are mainly composed of silicates. Organic content is low (<1% TOC), and diatoms are scarce. Carbonates are not present. Based on color and sediment composition, two subfacies can be identified. Facies 3a is brownish to dark grey, with relatively higher organic matter and diatom content. Facies 3b is lighter grey, and mainly composed of silicate material. Thin layers (0.5–1 cm thick) are only composed of Facies 3b. Other layers present a bottom layer of brown silty mud (Facies 3a) topped by homogeneous grey silty clays (Facies 3b). The thickest layer (92–104 cm) is composed of two light grey silty clay layers at bottom and top, and a thick, intercalated, brown silt layer.

The high organic matter and diatom contents, and the absence of carbonate and silicate components indicate that Facies 1 represents deposition in the open lacustrine realm of a eutrophic, freshwater lake without significant detrital input. The absence of laminated sediments suggests dominant oxic conditions at the lake bottom, and the presence of active bioturbation agents. Although salinity and lake level during deposition of these diatomaceous-rich sediments could have varied, the lacustrine system remained a freshwater lake, with high organic productivity, without authigenic carbonate formation, and lake levels similar to today's or even higher.

The high siliciclastic content, the presence of macrophyte rests and intraclasts, and the erosive nature of the lower contacts in Facies 2 indicate depositional conditions characterized by higher energy and therefore higher fluvial input. Such conditions would occur in the littoral environments of Laguna Aculeo and during flooding episodes reaching the deepest area of the lake. Thinner layers, associated with Facies 1, are more likely to represent mixed lacustrine and alluvial deposition in the central areas of the lake during flooding episodes. Thicker layers with higher

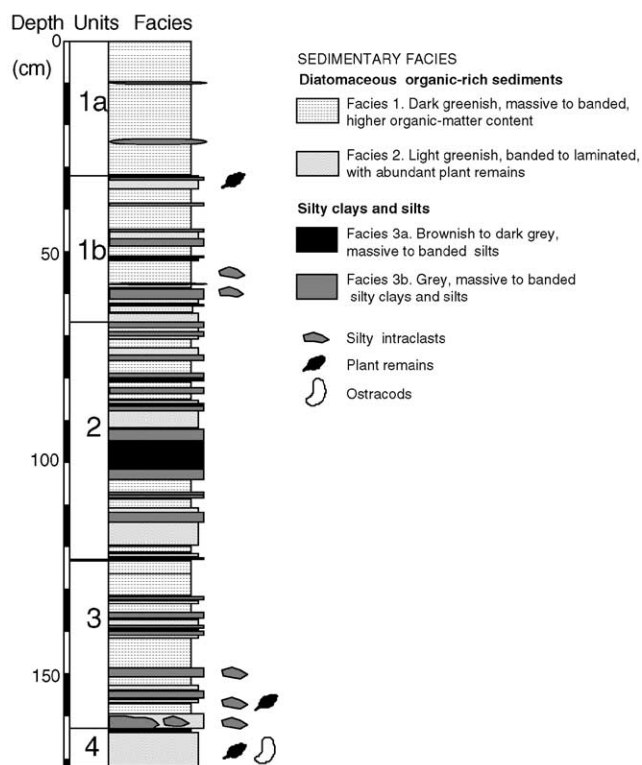


Fig. 3. Sedimentary facies and units identified in the Laguna Aculeo core.

carbonate content and presence of ostracods point to more littoral conditions, and, consequently, to low lake levels.

Facies 3 represents deposition in the central area of the lake during flooding episodes. Relatively higher organic matter content and more lacustrine sediment components in Facies 3b indicate reworking of littoral lacustrine sediments by floods. Facies 3a represents deposition of fine clastic material transported into the lake. The uniform silicate composition of the layers indicates that the sediment source was in the watershed. Sediments from the channels of the drainage network and the watershed would be mobilized during periods of extreme rainfall and high fluvial flows. Most of the coarse material transported by the creeks would be deposited in the shore areas of the lake, forming a small delta fan. The finer fraction (clay and silt size) would be transported as suspended load and reach the central area of the lake. Slow deposition would result in graded, fining-upward layers.

5.2. Chronology

In order to establish an accurate chronology, two independent dating methods, radiocarbon and ^{210}Pb were applied. The two cores were perfectly correlated using their magnetic susceptibility profiles and sedimentological descriptions. As the sedimentation rate varies significantly in the core, the time resolution is not constant through the section. In Unit 1, the time resolution ranges from annual to decadal, and a closer interval sample was chosen in order to detect changes during the last century. In the other units, time resolution provided by ^{14}C dates is of century scale, and the sampling interval is higher.

Radiocarbon dating was performed by AMS and conventional techniques (Table 2) and a 1-sigma (68.3%) confidence interval is indicated. Taking the southern Hemisphere correction into account, 24 years were subtracted (Stuiver et al., 1998b). The radiocarbon

dates were calibrated to calendar years with the Calib 4.1 program (Stuiver and Reimer, 1993; Stuiver et al., 1998a). In Table 2, ranges of the calibrated ^{14}C years are given for the 1-sigma (68.3%) confidence interval. No reservoir effect was detected for modern samples. The ^{14}C content of organic carbon from the first 10 centimeters of sediment was measured conventionally and yielded a value of 110.3 ± 0.8 pMC, corresponding to a modern age post-1963. The 172 cm core covers about the last 2000 years.

Unsupported ^{210}Pb activity was detected to a depth of 50 cm (Fig. 4). In general, the atmospheric activity signal of unsupported lead appears to have been largely diluted by episodes of rapid sedimentation in the upper part of the core. The ^{137}Cs activity versus depth profile has a well-defined sub-surface peak between 33 and 39 cm depth recording the 1964/1965 Southern Hemisphere fallout maximum from the atmospheric testing of nuclear weapons (Fig. 4). Comparison with the ^{210}Pb profile suggests that the shape of the ^{137}Cs peak was affected by an episode of rapid sedimentation during the early 1960s.

Because of the highly irregular ^{210}Pb profile, only the CRS dating model (Appleby and Oldfield, 1978) could be used to date the core, though the incomplete nature of the record made it necessary to use the ^{137}Cs date as a reference point (Oldfield and Appleby, 1984). Using this method, the mean ^{210}Pb flux to the sediments is estimated to be 48 ± 5 Bq/(m² yr). This is comparable with estimates of the atmospheric flux at this site and suggests that the ^{210}Pb record above 50 cm is relatively complete (Table 3, Figs. 4 and 5).

There is no date available between 50 and 113 cm. Because there is a large change in the sedimentation rate between Unit 1 and 2, linear interpolation between the two ages may not be realistic. Based on radiocarbon dates, the sedimentation rate seems to have been quite constant in both Units 2 and 3. Therefore, we calculated a regression line based on the ^{14}C dates of Units 2 and 3 (grey line). Subsequently, we extrapolated the chronology based on ^{210}Pb dates of Unit 1

Table 2
Overview of the radiocarbon dates^a

| Lab code | Depth (cm) | Sample code | ^{14}C age | $\delta^{13}\text{C}$ ‰ PDB | 1 σ max. age–min. age | Cal yr | Material |
|----------|------------|-------------|---------------------|-----------------------------|---|---------|-------------------------------|
| Hv 23487 | 0–10 | 1032-10 | > AD 1963 | –17.6 | ^{14}C content pMC 110.3 ± 0.8 | | Organic matter |
| Ua-15089 | 113–115 | 1101B-116 | 920 ± 65 | –29.6 | cal AD 1030–1220 | AD 1160 | Small wooden branch, charcoal |
| Hv 22728 | 115–117 | 1032-116 | 1065 ± 165 | –24.6 | cal AD 780–1190 | AD 1000 | Organic matter |
| OS-21743 | 145–146 | 1101B-150 | 1630 ± 55 | –28.5 | cal AD 410–540 | AD 430 | Wood |
| OS-21744 | 162 | 1101B-167 | 1800 ± 40 | –15.6 | cal AD 220–320 | AD 240 | Aquatic plants |
| Hv 22729 | 168–171 | 1032-169 | 2195 ± 95 | –22.9 | cal 380–60 BC | 200 BC | Organic matter |

^a Ua=Angstrom laboratory, Uppsala (AMS dating); OS=radiocarbon laboratory, Boulder (AMS dating); Hv=radiocarbon laboratory, Hannover (conventional radiocarbon dating). Dates were corrected for the southern Hemisphere, calibrated with Calib 4.1 (Stuiver et al., 1998a) and based on the 1-sigma confidence interval (68.3%).

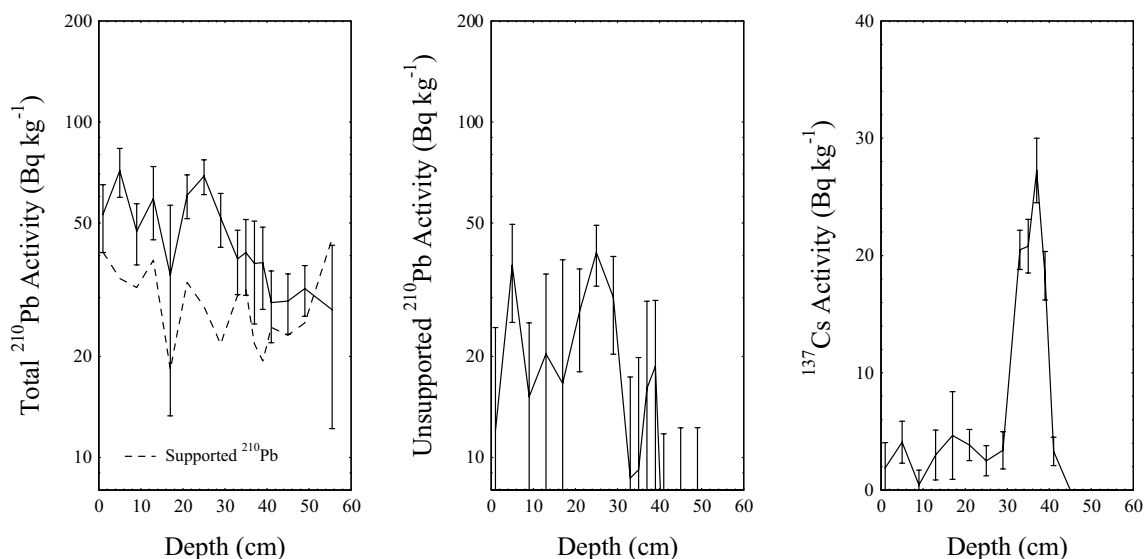


Fig. 4. ^{210}Pb and ^{137}Cs dates for the chronology. Fallout radionuclide concentrations versus depth showing: (a) total and supported ^{210}Pb ; (b) unsupported ^{210}Pb ; (c) ^{137}Cs . A very pronounced caesium peak was detected.

Table 3
 ^{210}Pb chronology

| Depth (cm) | (g/cm ²) | Chronology | | | Sed. rate (g/(cm ² yr)) |
|---------------|----------------------|--------------|-------------|---|---------------------------------------|
| | | Date (AD) | Age (yr) | ± | |
| 0.0 | 0.0 | 1998 | 0 | 0 | |
| 1.0 | 0.2 | 1998 | 0 | 1 | 0.30 |
| 3.0 | 0.4 | 1997 | 1 | 1 | 0.20 |
| 5.0 | 0.5 | 1996 | 2 | 2 | 0.19 |
| 7.0 | 0.7 | 1995 | 3 | 2 | 0.17 |
| 9.0 | 0.9 | 1994 | 4 | 2 | 0.20 |
| 11.0 | 1.1 | 1993 | 5 | 2 | 0.23 |
| 13.0 | 1.3 | 1992 | 6 | 2 | 0.22 |
| 15.0 | 1.6 | 1991 | 7 | 2 | 0.21 |
| 17.0 | 1.8 | 1990 | 8 | 3 | 0.18 |
| 19.0 | 2.0 | 1988 | 10 | 3 | 0.16 |
| 21.0 | 2.2 | 1987 | 11 | 3 | 0.11 |
| 23.0 | 2.5 | 1984 | 14 | 4 | 0.09 |
| 25.0 | 2.8 | 1980 | 18 | 4 | 0.08 |
| 27.0 | 3.2 | 1975 | 23 | 4 | 0.07 |
| 29.0 | 3.5 | 1970 | 28 | 4 | 0.08 |
| 31.0 | 3.8 | 1967 | 31 | 4 | 0.11 |
| 33.0 | 4.0 | 1965 | 33 | 4 | 0.13 |
| 35.0 | 4.2 | 1964 | 34 | 4 | 0.15 |
| 37.0 | 4.4 | 1962 | 36 | 4 | 0.10 |
| 39.0 | 4.6 | 1960 | 38 | 5 | 0.11 |
| 41.0 | 4.9 | 1958 | 40 | 5 | 0.19 |
| 43.0 | 5.3 | 1957 | 41 | 6 | 0.25 |
| 45.0 | 5.6 | 1955 | 43 | 6 | 0.21 |
| 47.0 | 6.0 | 1953 | 45 | 7 | 0.18 |
| 49.0 | 6.4 | 1951 | 47 | 8 | 0.18 |

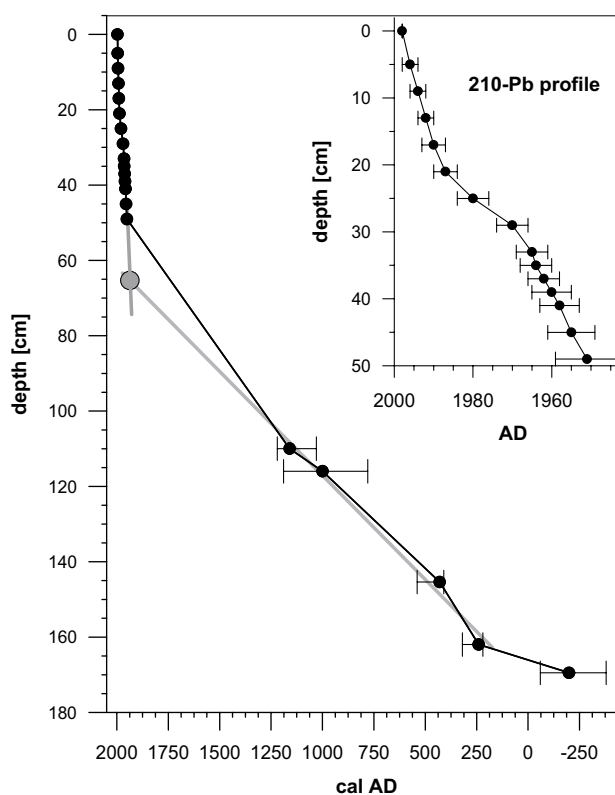


Fig. 5. Age–depth model of the Laguna Aculeo core. ^{210}Pb dates cover the last 50 years. Radiocarbon years are calibrated using Calib 4.1 (see Table 2). The error bars are based on a 1-sigma confidence interval (see text for further explanation).

down-core (grey line, Fig. 5). The point of intersection of the two extrapolations lies between 65 and 70 cm, close to the limit between sedimentary Units 1 and 2 (at 66 cm depth). Hence, we ascribed AD 1930 to the

intersection point for further interpretation. The good agreement between the two independent chronologies supports the robustness of the chronological framework for the Laguna Aculeo core.

5.3. Magnetic susceptibility

Magnetic susceptibility is a complex parameter mainly controlled by mineralogy, grain size, sediment density and organic carbon percentage. Magnetic susceptibility values of wet bulk sediment in Laguna Aculeo core show a distinctive pattern (Fig. 6): low values in Unit 4 and 3 (172–122 cm); high values in Unit 2 (122–66 cm); relatively low and decreasing values in the lower section of Unit 1 (66–30 cm) and low values at the top of the core (30–0 cm). The main peaks correlate well with the occurrence of siliclastic layers (Facies 3). Some of the very thin clastic intervals do not show up in the magnetic susceptibility record because the measurements average about 2 cm. The decrease in magnetic susceptibility in the upper 66 cm may not indicate lower clastic input. The high water and oxygen content of these upper sediments, and the presence of other sediment components such as organic matter, biogenic silica and carbonates that give weak or even negative values of magnetic susceptibility seem to have diluted the signal and caused low magnetic susceptibility values. Therefore, mass specific measurements would provide more precise values in the uppermost sediments. Magnetic susceptibility peaks also correlate well with low water content, high wet bulk density and the presence of clastic layers.

5.4. Geochemistry

Geochemical compositions of selected major and trace elements provide information about sediment sources and past limnological changes. Calcium and strontium cations are related to the carbonate fraction of the sediments (Fig. 7). The correlation of calcium and strontium values with the carbonate content indicates that carbonates are the main source of those cations. Carbonate content in the core sediments is practically zero, and there are only two intervals with significant percentages (around 10%) at 163–172 and 30–40 cm. As carbonate rocks are absent in the catchment (Fig. 1), the calcium carbonate occurring in the sediments must be formed in the lake. These intervals, characterized by deposition of the mainly littoral Facies 2, occurrence of calcium carbonate, and higher Ca and Sr concentrations, reflect low lake levels with increased ion concentration of the lake water.

The potassium, aluminum and magnesium cations are provided by the silicate sediment fraction. The K and Mg are also adsorbed by clay minerals after weathering of volcanic and plutonic rocks in the catchment (Fig. 1). Aluminum is primarily allogenic in most lakes and usually viewed as an indicator of clastic input and erosion intensity in the watershed (Engstrom and Wright, 1984). Because the chemical method used primarily extracts adsorbed cations from clay minerals,

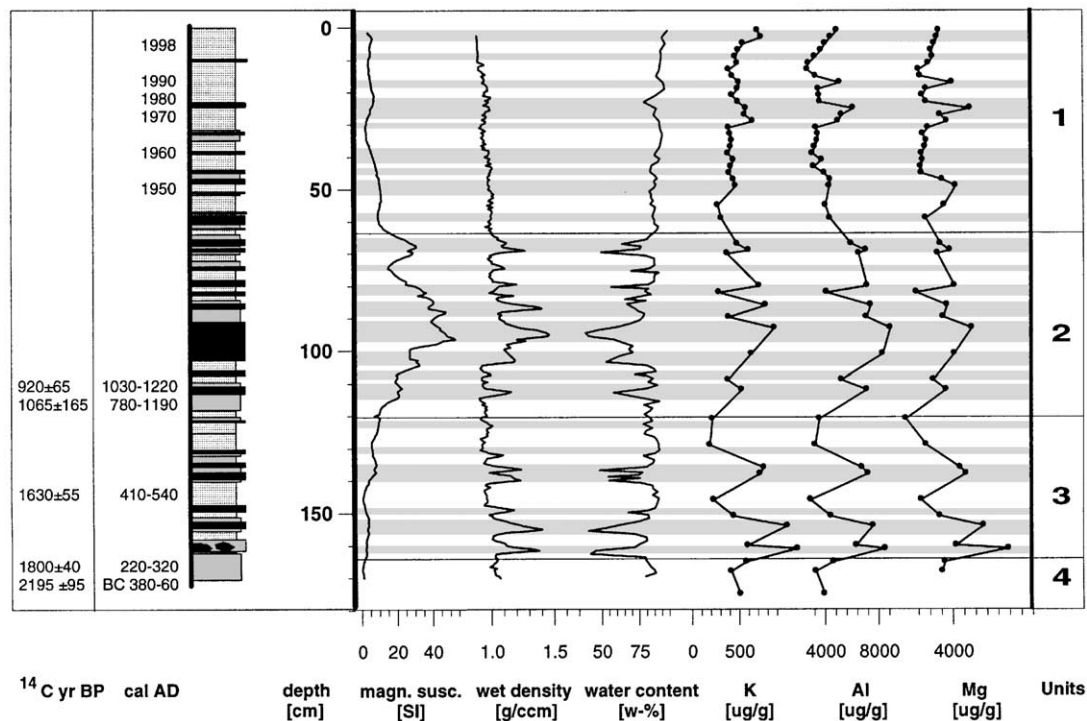


Fig. 6. Sedimentological and geochemical data for the last 2000 years. Flood events are indicated by sedimentary facies, as well as physical and geochemical parameters (see text for explanation).

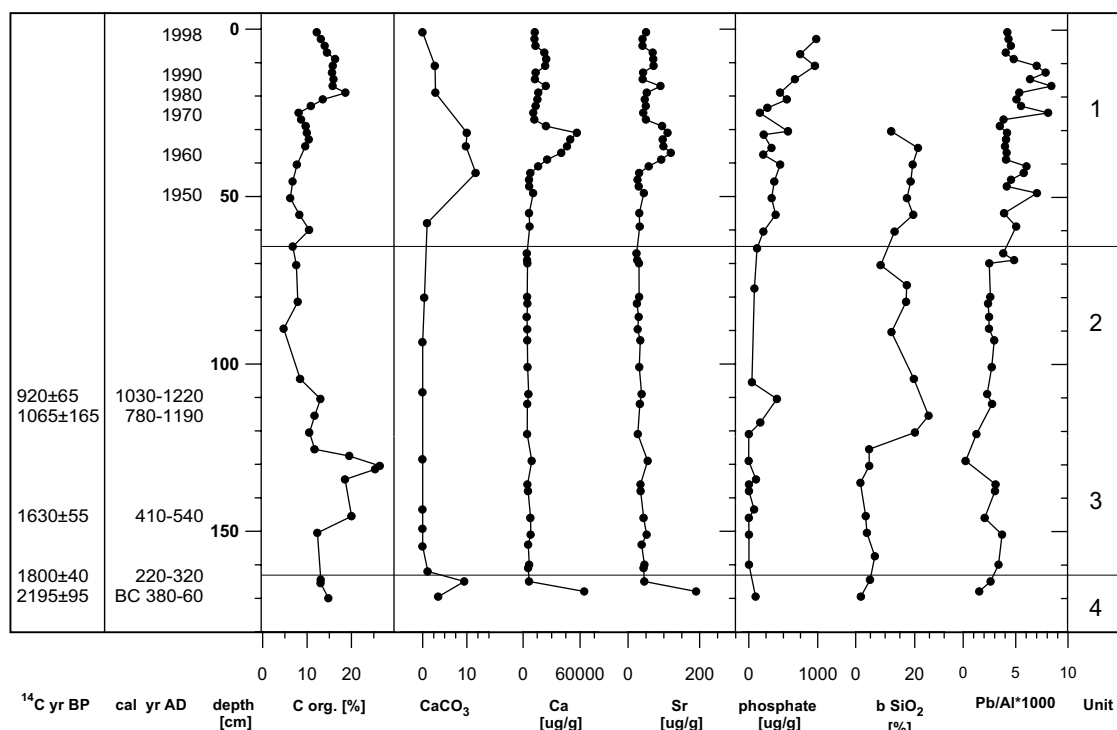


Fig. 7. Humidity changes and human impact during the late Holocene. Two probably drier periods (around cal 200 BC–AD 200 and in the late 1960s) are indicated by high carbonate, Sr and Ca contents. Moreover, high biogenic silica and phosphate contents are indicators of recent eutrophication. For phosphate, organic carbon and biogenic silica, no samples from clastic layers (Facies 3) were included in the measurements.

the K and Mg profiles can also be considered as proxies for clay content. Increased soil erosion in the watershed, and higher alluvial influx in the lake would cause higher Al, K and Mg content in the sediments (Mackereth, 1966). Magnesium, however, also occurs in carbonates. The carbonate concentration, though, is very low, except for the two identified intervals with low Mg concentrations (Fig. 7). Therefore, carbonates can be considered as a negligible magnesium source. Overall, K, Mg and Al curves are indicators of siliciclastic content of the sediments and reflect the intensity of erosion in the catchment. The three curves show similar profiles (Fig. 6): low values in Unit 4, high values at the bottom, and generally decreasing values in Unit 3, high values in Unit 2, and relatively constant and low values in Unit 1. In general, the clastic layers (Facies 3) correlate very well with the high magnetic susceptibility and density, low water content and high amounts of potassium, aluminum and magnesium.

Biogenic silica content shows low values ranging from 1% to 7% below 120 cm (Fig. 7). At the beginning of Unit 2, there is a sudden increase in silica content up to 25%. Values remain mostly higher than 15% in the upper part of the sediment core. Phosphate content is very low but shows a dramatic increase in the uppermost sediments (Fig. 7). The analytical technique used does not discriminate among the three types of phosphate

occurring in lake environments: (i) discrete mineral phases; (ii) inorganic authigenic phases and (iii) authigenic phosphorus bound to organic compounds (Engstrom and Wright, 1984). However, mineral input can be neglected, as smear slides do not show apatite or vivianite. Therefore, phosphate content can be mainly related to authigenic phosphate, which is a potential proxy for trophic conditions in the past (Engstrom and Wright, 1984). Detrital phosphate minerals do not contribute to primary productivity.

Lead values were close to the detection limit, and an uncertainty of about 15% should be taken into consideration (Fig. 7). To eliminate variations due to clastic accumulation, lead content is standardized using aluminum. Several studies have used Al as a conservative element against which variations in the accumulation of anthropogenic input can be compared (e.g. Kemp et al., 1976). The Pb/Al curve shows a marked increase of Pb in the upper 70 cm.

5.5. Diatoms

A total of 57 diatom taxa were identified (Table 4). Most taxa are benthic or epontic (ca. 80%) and only about 20% are euplanktonic or tychoplanktonic. The most abundant taxa are *Aulacoseira granulata* (5–90%), *Melosira pseudogranulata* (1–55%), *Cyclotella*

Table 4

List of all 57 diatom taxa identified in the core

| | |
|---|---|
| <i>Achnanthes</i> | <i>constrictum</i> Ehrenberg |
| <i>lanceolata</i> (Breb.) Grunow | <i>gracile</i> Ehrenberg |
| <i>hungarica</i> Grunow in Cleve et Grun | <i>martini</i> Fricke |
| <i>Amphora</i> Ehrenberg | <i>parvulum</i> (Kützing) Kützing |
| <i>veneta</i> Kützing | sp. |
| <i>Aulacoseira</i> Agardh | <i>Gyrosigma</i> Hassall |
| <i>granulata</i> (Ehrenberg) Simonsen | <i>spencerii</i> (Quekett) Griffith et Henfrey |
| <i>Bacillaria</i> J.L. Gmelin | <i>Hantzschia</i> Grunow |
| sp. | <i>amphioxys</i> (Ehrenberg) Grunow |
| <i>Cocconeis</i> Ehrenberg | <i>Melosira</i> C.A. Agardh |
| <i>placentula</i> var. <i>euglypta</i> (Ehrenberg) Grunow | <i>pseudogranulata</i> Cleve-Euler |
| <i>Craticula</i> Grunow | <i>Navicula</i> Bory |
| <i>cuspidata</i> (Kützing) Mann | <i>lanceolata</i> (Agardh) Ehrenberg |
| <i>Cyclotella</i> (Kützing) Brébisson | <i>salinarum</i> Grunow in Cleve et Grunow |
| <i>meneghiniana</i> Kützing | <i>viridula</i> (Kützing) Ehrenberg |
| <i>operculata</i> (Agardh) Kützing | <i>Neidium</i> Pfitzer |
| <i>stelligera</i> (Cleve and Grunow) Van Heurck | <i>iridis</i> (Ehrenberg) Cleve |
| <i>Cymatopleura</i> W. Smith | <i>Nitzschia</i> Hassall |
| <i>solea</i> (Brébisson) W. Smith | <i>acicularis</i> (Kuetzing) W. Smith |
| <i>Cymbella</i> Agardh | <i>amphibia</i> Grunow |
| <i>affinis</i> Kützing | <i>frustulum</i> (Kuetzing) Grunow |
| <i>difficilis</i> Krasske | <i>palea</i> (Kuetzing) W. Smith |
| <i>lanceolata</i> (Agardh) Agardh | <i>philippinarum</i> Hustedt |
| <i>tumida</i> (Brébisson) Van Heurck | <i>substratoides</i> |
| <i>Denticula</i> F.T. Kuetzing | <i>Pinnularia</i> Ehrenberg |
| sp. | <i>brevicostata</i> Cleve var. |
| <i>Diatoma</i> Bory | <i>divergens</i> W. Smith |
| <i>vulgare</i> Bory | <i>gibba</i> Ehrenberg |
| <i>Encyonema</i> F.T. Kuetzing | <i>major</i> (Kützing) Rabenhorst |
| <i>minutum</i> (Hilse in Rabh.) D.G. Mann | <i>Sellaphora</i> Mereschkowsky |
| <i>Epithemia</i> Brébisson | <i>pupula</i> (Kützing) |
| <i>adnata</i> (Kützing) Brébisson | <i>Stauroneis</i> Ehrenberg |
| <i>sorex</i> Kützing | <i>phoenicenteron</i> (Nitzsch) Ehrenberg <i>anceps</i> |
| <i>Eumotia</i> Ehrenberg | (Lewis) Brébisson ex Van Heurck |
| <i>pectinalis</i> (Dyllwyn) Rabenhorst | <i>Staurosira</i> Ehrenberg |
| <i>Fragilaria</i> Lyngbye | <i>construens</i> Ehrenberg |
| <i>capucina</i> Dezmaizeres | <i>Staurosirella</i> Williams and Round |
| <i>crotonensis</i> Kitton | <i>pinnata</i> (Ehrenberg) Williams and Round |
| <i>Geissleria</i> Lange–Bertalot and Metzeltin | <i>leptostauron</i> (Ehr.) Williams and Round |
| <i>decussis</i> (Østrup) Lange–Bertalot and Metzeltin | <i>Synedra</i> Ehrenberg |
| <i>Gomphonema</i> Agardh | <i>acus</i> Kuetzing |
| <i>affine</i> Kuetzing | <i>rumpens</i> Kuetzing |
| <i>angustatum</i> (Kützing) Rabenhorst | <i>ulna</i> (Nitzsch) Ehrenberg |

operculata (1–21%) and *Staurosira construens* (1–25%). Those taxa reaching a relative abundance of 2% in at least one sample are shown in Fig. 8.

In Unit 4, *Amphora veneta* shows the highest percentage with almost 30%. Van Dam et al. (1994) classify the *Amphora veneta* as a brackish water species. On the other hand, Cholnoky (1968) emphasizes that *Amphora veneta* is not especially a brackish water species but an inhabitant of strongly alkaline waters. But *Nitzschia frustulum* also appears to be described as a true brackish water diatom by Cholnoky (1968). In addition, *Gomphonema affine*, *Gomphonema gracile* and *Gomphonema parvulum* also show rather high percentages. They all indicate higher salinity. The taxa

Aulacoseira granulata seldom occurs, compared to the other units.

In Unit 3, the abundance of the species *Aulacoseira granulata* (TP optimum 29 µg/l, Dixit et al., 1999) gradually increases from about 50% to 70%. Moreover, maximum abundance of the eutrophic species *Staurosira construens* and *Staurosirella pinnata* (TP optimum 16.5 and 15 µg/l, respectively, Cumming et al., 1995) occurs at a depth of 120 cm, but is based on a single sample. The oligotrophic species *Cyclotella stelligera* (TP optimum 7–9.7 µg/l, Denys, 1991) and the mesotrophic species *Gomphonema affine* and *Gomphonema gracile* (Van Dam et al., 1994) are also abundant. The brackish water indicators (*Nitzschia frustulum*, *Amphora veneta*,

the deposition of littoral sediments (Facies 2 and abundance of marsh plant remains), and the high carbonate, Ca and Sr concentrations. The exclusive presence of ostracods in this unit favors more carbonate-enriched waters. During deposition of Unit 4, Laguna Aculeo was shallower than today, and its surface area was likely to be reduced, with a wetland or marsh complex surrounding the lake. Relatively high organic matter content seems related to higher productivity in the littoral and marshy areas. Since floods are more likely to reach the center of the lake when lake levels are low, the absence of siliciclastic layers suggests that flooding events were rare during this period.

Unit 3 (163–122 cm, cal AD 200–950) was deposited in a freshwater lake, with no authigenic carbonate formation, and with high organic productivity (TOC between 10% and 30%). The lake transgression is marked by a reworked layer (163–160 cm) with abundant silty and diatomaceous-rich soft sediment intraclasts. The dominance of banded diatomaceous sediments suggests a higher lake level than in Unit 4. Saline indicator diatom species (*Amphora veneta*, *Gomphonema affine* and *Gomphonema gracile* and *Gomphonema parvulum*) show a lower abundance than in Unit 4, although freshwater taxa dominate. The presence of both saline and freshwater taxa could reflect periods of lake stratification. Siliciclastic layers (Facies 3) are abundant and are reflected by high magnetic susceptibility, density, K, Al and Mg concentrations as well as low water content. There are two periods of higher frequency of clastic layers, the first around cal AD 200–400 and the second around cal AD 500–700. Thus in the past, as in today's climatic conditions, increased winter precipitation would be responsible for flooding events.

Unit 2 (122–66 cm, cal AD 950–1930) is characterized by the presence of numerous siliciclastic layers (Facies 3). The frequency of flooding events is greater than before, with more than 10 during about 1000 years. Also, the highest magnetic susceptibility values of the core point to increased clastic input. Based on the different thickness of Facies 3 layers, the intensity of the flooding events was variable. Organic matter content is lower than in Unit 3, generally not exceeding 10%, which would suggest lower lacustrine organic productivity. However, the large increase in biogenic silica from 5% to 20% at the base of Unit 2 (around cal AD 950) would indicate greater productivity in the lake, as well as higher humidity.

Absence of carbonates points to a freshwater lake, with chemistry similar to that of Unit 3. The dominance of the littoral Facies 2 with respect to deeper-water Facies 1 could indicate relatively lower lake levels. On the other hand, this could be a reflection of higher energy due to the flooding events. Moreover, the saline indicator diatoms (*Amphora veneta*, *Gomphonema affine* and *Gomphonema gracile* and *Gomphonema parvulum*)

that are abundant in Unit 3 and 4 virtually disappear in Unit 2, suggesting freshwater conditions.

Unit 1 (66–0 cm, about AD 1930–1998) is dominated by diatomaceous muds (Facies 1). Deposition of the littoral Facies 2, corresponding to high calcium carbonate, Ca and Sr values, in the 30–40 cm interval, indicates a period of increased lakewater concentration and probably lower lake levels. This period occurred between 1960 and 1970 and it seems to correspond to the late 1960s when rainfall was low (Fig. 2a). At that time, several areas of the lake emerged, and horseback rides had become possible through the eastern side of the lake (pers. comm. Letelier, 1998). Although discrete siliciclastic layers are partly diluted, there is clear evidence of periods of increased fluvial input and higher energy deposits. Moreover, flood events are also defined by their geochemical signature: higher concentrations of Al, Mg and K. Based on these different proxies, at least eight flood events were detected during the period AD 1950 and 1998. According to the ^{210}Pb chronology, these events occurred around AD 1997, 1993–1995, 1989–1992, 1978–1987, 1959–1966 and 1950–1953. A standard deviation of ± 1 year at AD 1997 up to ± 8 years at AD 1950, respectively, has to be considered (Table 3). These periods correspond to years with annual precipitation higher than 600 mm, which represent mainly the El Niño years.

The upper sediments show strong human impact on the lake ecosystem related to tourism and agriculture. Tourism started in the 1960s, with the construction of weekend lakeshore houses (pers. comm. Letelier, 1999). Sewage and agricultural discharge turned the lake into a eutrophic system. Cabrera and Montecino (1982) found severe O_2 depletion on the bottom of the lake, and detected sporadic fish mass mortality events, all pointing to highly eutrophic conditions. In the sediments of Laguna Aculeo, phosphate and organic matter contents increased, and eutrophic diatom species became more abundant, though there are some uncertainties concerning the interpretation of the diatom *Melosira pseudogranulata*. Sedimentation rate increased as well, which is a phenomenon typical for eutrophic lakes. The increase of lead in recent times points to human impact, probably due to the use of fossil fuels in the region. Nowadays, the Laguna Aculeo is a highly disturbed and eutrophic system (Cabrera and Montecino, 1982).

6.2. Climate evolution of the last 2000 years in Central Chile

For the last 2000 years, the limnological changes in Laguna Aculeo provide new information about climate variability in Mediterranean Central Chile. The driest period recorded in the Laguna Aculeo core occurred between about cal 200 BC to AD 200 (Unit 4). Around cal AD 200, a lake transgression took place and

dominant freshwater conditions were established. The late Holocene seems to have been humid compared to the entire Holocene in the lowlands of Central Chile. The onset of this humid phase is also indicated in other sites in the region. Villagrán and Varela (1990) describe a change to more humid conditions with the recolonization of arboreal taxa around cal AD 360 (1720 ± 80 ^{14}C yr BP), based on a pollen profile in the Quintero peat bog ($32^\circ 47'\text{S}$). Villa-Martínez and Villagrán (1997) describe the appearance of arboreal taxa earlier, around cal 50 BC (cal 210 BC–AD 80 (1-sigma), 2060 ± 70 ^{14}C yr BP) in the same peat bog. Because the ^{14}C chronology is based on total organic carbon samples, a reservoir effect is possible and it could explain the slightly greater age compared to Laguna Aculeo. The period between about cal AD 200 and 950 (Unit 3) represents a period of relatively high lake levels and high organic productivity. Abundant siliclastic layers in the sediment reflect repeated large flood events. In order to detect periods with different frequencies of clastic events, the data were plotted against a calibrated time scale (Fig. 9). There are four main periods with a high frequency of flood events: around cal AD 200–400, 500–700, 1300–1700 (with the greatest frequency of flood events around cal AD 1400–1600) and 1850–1998. The Laguna Aculeo record suggests a complex pattern of climate variability in the region during the Little Ice Age. The period of increased moisture from cal AD 1300–1700

was followed by a period of less frequent and intense flood events (AD 1700–1850) and a subsequent increase afterwards.

The moisture in Central Chile comes directly from the west over the Pacific Ocean. Increased precipitation and erosion rates in the watershed of Laguna Aculeo would be a response to stormier winters. Hence, enhanced Westerlies and frontal system activity during the winter and a weakened southeast Pacific high-pressure cell seem to be responsible for the abundant flooding events. The earliest period with repeated flood events (cal AD 200–400) might correspond to more humid conditions in the Norte Chico ($27\text{--}33^\circ\text{S}$), roughly around cal AD 0–400 based on pedological evidence (Veit, 1996).

Around cal AD 950–1930 (Unit 2), the frequency and intensity of the flood events increased even more, with more than 10 flood layers in about 1000 years. This is especially true for the periods from about cal AD 1300–1700 and 1850–1930, when high magnetic susceptibility of the core indicates a high frequency of flood events. Some of the clastic layers may include more than one flood event, so the total number could even be higher. During that time, the saline indicator diatom species virtually disappeared, also suggesting freshwater conditions.

In the Norte Chico ($27\text{--}33^\circ\text{S}$), Veit (1996) also considers the period around cal AD 1300–1800 a period of increased humidity due to the Westerlies. Röthlisberger (1986) dated two glacier advances at

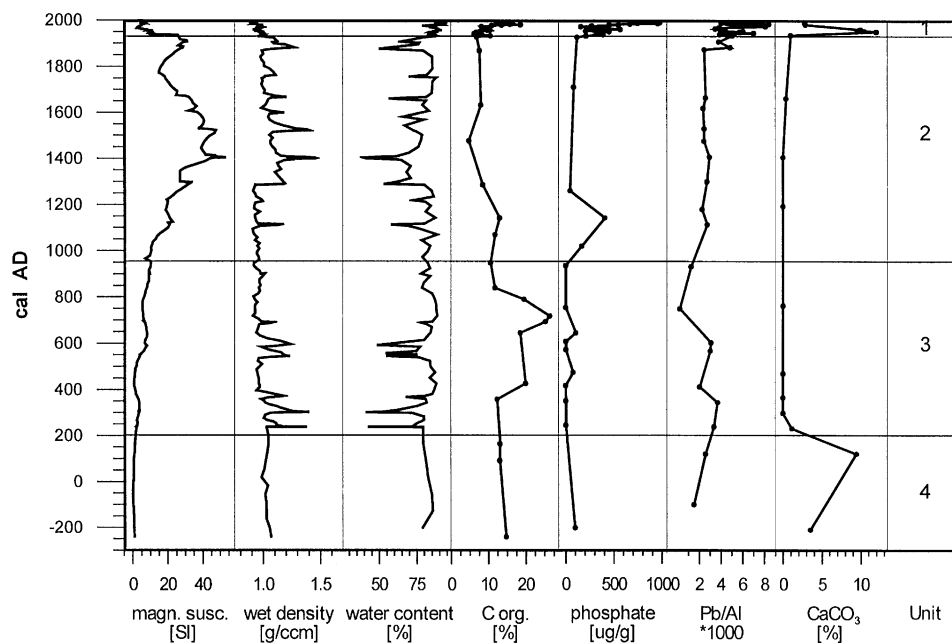


Fig. 9. Climate change during the last 2000 years on the calibrated time scale. All ^{210}Pb as well as calibrated radiocarbon dates are included. The terrestrial macrorests are preferred to the bulk sediment only at a depth of 115 cm, where two dates overlap. For calculation of the calibrated age scale, the thickness of the flood layers (Facies 3) was subtracted, because they were deposited very rapidly compared to the “normal” sedimentation rate. In general, quite humid conditions persisted during the last 2000 years. Abundant flood layers, especially during the Little Ice Age, are well represented by high magnetic susceptibility and density and low water content. Two drier periods, about 2000 years ago and in the late 1960s, are represented, e.g. by higher carbonate contents. Increase in lead and phosphate concentration points to a probable human impact in the 20th century.

34°S, at the beginning of the 14th century and around AD 1860, respectively. Two cold pulses have been identified in the central regions of Argentina during the Little Ice Age (Cioccale, 1999): from the 15th to the 16th century and from the beginning of the 18th century until the beginning of the 19th century. The first period roughly corresponds with the periods in the Laguna Aculeo record of the greatest frequency of flood events (around cal AD 1400–1600). Further south, in northern Patagonia, a region influenced exclusively by the Westerlies, Villalba (1994b) describes tree ring records showing a cold-moist period between cal AD 1270 and 1670. Dendrochronological records in the mid-latitudes of South America (30–45°S) in general, show precipitation above the long-term mean from cal AD 1450–1550 and 1840–1900, and extended droughts from cal AD 1570–1650 and 1770–1820 (Lara and Villalba, 1993; Villalba, 1994a, b). The humid period from cal AD 1450–1550 might roughly correspond to the period of very high intensity of flood events around cal AD 1400–1600 in Laguna Aculeo (Fig. 6). These collective data support the hypothesis of intensified Westerlies as the main reason for increased precipitation in Central Chile and the Norte Chico. The record of Laguna Aculeo therefore provides a regional climate signal.

The influence of the Westerlies diminishes to the north and the tropical circulation dominates as the main moisture source. Concerning the late Holocene, a lake study of Grosjean et al. (1997) at 27°S in the Norte Chico points to an increase in moisture after about 4000 cal yr BP suggesting increased precipitation from the Westerlies. Further north, however, at about 24°S on the Chilean Altiplano, the late Holocene moisture increase appears to be mainly related to the tropical circulation belt (Valero-Garcés et al., 1996). Studies of Lake Titicaca (16°S) support a dry mid-Holocene period, but an increase around 4000 cal yr BP (Cross et al., 2000; Wirmann and Mourguiart, 1995). An increase in humidity in the late Holocene is also seen in the Sajama ice core indicated by a subsequent decrease in aerosols from 3000 cal yr BP to the present (Thompson et al., 1998). The authors suggest that the Amazon River basin had remained the dominant moisture source for the tropical Andes. Regional differences and local factors may explain some records showing increased moisture during the mid-Holocene in the Atacama region (Betancourt et al., 2000). Most of the records suggest that Central Chile as well as the Altiplano appear to have been very dry in the mid-Holocene, and that humidity generally increased in the late Holocene. However, the moisture sources in both regions are very different. Markgraf (1998) indicates for the Westerlies in Central Chile that modern seasonal shifts of the storm tracks became established only during the last 4000 years when insolation seasonality began to increase.

Like Central Chile, northern Peru is also characterized by high precipitation during El Niño events (e.g. Wells, 1990; Markgraf, 1998). At the Quelccaya ice cap (Peru), a site only influenced by tropical air masses, precipitation was higher during the period cal AD 1500–1750 and greatly reduced afterwards until AD 1860 (Thompson et al., 1984). There is some evidence, albeit not conclusive, that there were more frequent and stronger El Niño events compared to the previous period (Quinn et al., 1987; Anderson, 1992). Moreover, Aceituno and Montecinos (1992) state that the relationship between the southern oscillation index (SOI) and rainfall in Central Chile is clearly positive, but has varied significantly during at least the 20th century with the highest correlation around 1950 suggesting changes in how the SOI operates. The positive correlation of El Niño and high rainfall producing flood layers in Laguna Aculeo seems to characterize the last 50 years. Based on the ²¹⁰Pb chronology, the high flood frequency periods occurred around AD 1997, 1993–1995, 1989–1992, 1978–1987, 1959–1966 and 1950–1953. All years with annual precipitation above 600 mm and almost all El Niño years are represented by those periods of flooding (Fig. 2a). But before that period, the resolution of the record of Laguna Aculeo is not high enough to show evidence for a strong relationship between ENSO and flood layers. Focusing on the entire Holocene, it appears that prior to about 5500 cal yr BP, ENSO was probably greatly reduced or even not functioning (e.g. Keefer et al., 1998; Sandweiss et al., 1999). Interestingly, the mid-Holocene represents a very dry period in Mediterranean Central Chile (Heusser, 1983; Villagrán and Varela, 1990). According to Markgraf (1998), ENSO may actually imply overall higher levels of precipitation, despite the increased variability, in northern Peru, Ecuador and Central Chile.

7. Summary and conclusions

A multi-proxy study based on sedimentology, geochemistry and diatoms of a 172 cm core from Laguna Aculeo (33°50'S) sediments provides detailed information about moisture changes in Mediterranean Central Chile during the last 2000 years. The lake lies just at the northern border of strong Westerly influence with dry summers and humid winters. Clastic layers deposited in the lake during floods seem to be strongly correlated with winter rains from the Westerlies. Comparison with other archives in Central Chile indicates that this site shows a regional palaeoclimate signal.

In general, humid conditions persisted during the last 2000 years compared to the entire Holocene. Our record of past moisture balance in Mediterranean Central Chile starts around cal 200 BC with the driest conditions persisting until about cal AD 200. Subsequently, a high

lake level was established due to more humid conditions. There are four main periods with a great frequency of clastic layers reflecting floods: around cal AD 200–400, 500–700 and cal AD 1300–1700, with a main peak around cal AD 1400–1600, and 1850–1998. These periods indicate an increased intensity of Westerlies with more frontal system activity during winter and a weakened southeast Pacific high-pressure cell, probably comparable to modern conditions. During the last 50 years, at least eight flood events were detected covering most El Niño years.

Overall, palaeoclimatic data in Mediterranean Chile are still scarce and more paleorecords from different archives are needed to draw a detailed history of Holocene changes of the Westerlies. Furthermore, although the close relationship of ENSO and high precipitation events in the region is obvious, more evidence is needed for the entire Holocene in order to discuss the question whether ENSO was weakened or disappeared during the mid-Holocene, as interpreted for example in northern Peru.

Acknowledgements

This study was funded by the Swiss National Science Foundation (NSF 21-50854.97 and 20.56908.99). We would like to thank Daniel Ariztegui, Platt Bradbury, Erika Gobet, Martin Grosjean, Philip Jeker, Urs Krähenbühl, Moritz Lehmann, and Frank Oldfield for scientific support and fruitful discussions, and Andreas Brodbeck for the cartography. We are grateful to Caspar Ammann for his critical editorial support. We thank Willi Tanner, Martin Grosjean, Christoph Lucas, Julieta Massafiero and Rodrigo Villa for help during fieldwork and Fernando Escobar (DGA, Chile) for providing part of the climate data. We also appreciate the critical and helpful reviews by Vera Markgraf and Florence Sylvestre.

In addition, we are grateful to the Limnological Research Center (University of Minnesota, Minneapolis, USA) and the Swiss Laboratories of Chemistry and Botany (University of Bern) and Limnogeology (ETH Zürich) for lab facilities and the radiocarbon Laboratory in Boulder for providing AMS dates at the reduced IAI rate.

References

Aceituno, P., 1989. On the functioning of the southern oscillation in the South American sector. Part II: upper-air circulation. *Journal of Climate* 2, 341–355.

Aceituno, P., Montecinos, A., 1992. Analisis de la estabilidad de la relación entre la oscilación sur y la precipitación en America del Sur. Palaeoenso-records, International Symposium, Orstom-Conicet, Lima, pp. 7–13.

Anderson, R., 1992. Long-term changes in the frequency and occurrence of El Niño events. In: Diaz, H., Markgraf, V. (Eds.), *El Niño, Historical and Paleoclimatic Aspects of the Southern Oscillation*. Cambridge University Press, Cambridge, pp. 193–200.

Appleby, P.G., Oldfield, F., 1978. The calculation of ^{210}Pb dates assuming a constant rate of supply of unsupported ^{210}Pb to the sediment. *Catena* 5, 1–8.

Appleby, P.G., Nolan, P.J., Gifford, D.W., Godfrey, M.J., Oldfield, F., Anderson, N.J., Battarbee, R.W., 1986. ^{210}Pb dating by low background gamma counting. *Hydrobiologia* 141, 21–27.

Betancourt, J.L., Latorre, C., Rech, J.A., Quade, J., Rylander, K.A., 2000. A 22,000-year record of monsoonal precipitation from Northern Chile's Atacama desert. *Science* 289, 1542–1546.

Boninsegna, J.A., 1990. Santiago de Chile winter rainfall since 1220 as being reconstructed by tree rings. *Quaternary of South America and Antarctic Peninsula* 6, 67–87.

Cabrera, S., Montecino, V., 1982. Eutrophy of lake Aculeo. *Plant and Soil* 67, 377–387.

Campos, H., Steffen, W., Aguero, G., Parra, O., Zuñiga, L., 1992. Limnological studies of lake Rupanco (Chile), morphometry, physics, chemistry, plankton and primary productivity. *Archiv fuer Hydrobiologie* 90 (Suppl.), 85–113.

Cholnoky, B.J., 1968. *Die Oekologie der Diatomeen in Binnengewässern*. Cramer, Berlin, p. 699.

Cioccale, M.A., 1999. Climatic fluctuations in the central region of Argentina in the last 1000 years. *Quaternary International* 62, 35–47.

Cleve-Euler, A., 1948. Suesswasserdiatomeen aus dem Feuerland. *Acta geografiska Helsingt* 10 (1), 61.

Corvalán, J., Munizaga, F., 1972. Edades radiométricas de rocas intrusivas y metamórficas de la Hoja Valparaiso—San Antonio. Chile. *Instituto de Investigaciones Geológicas* 29, 1–40.

Cross, S.L., Baker, P.A., Seltzer, G.O., Fritz, S.C., Dunbar, R.B., 2000. A new estimate of the Holocene lowstand level of Lake Titicaca, central Andes, and implications for tropical palaeohydrology. *The Holocene* 10 (1), 21–32.

Cumming, B., Wilson, S., Hall, R., Smol, J., 1995. Diatoms from British Columbia (Canada) lakes and their relationship to salinity, nutrients and other limnological variables. Cramer, Berlin, p. 207.

Denys, L., 1991. A check-list of the diatoms in the Holocene deposits of the Western Belgian coastal plain with a survey of their apparent ecological requirements. Introduction, ecological code and complete list. *Belgische Geologische Dienst Brussels prof paper* 246, 1–41.

Dixit, S.S., Smol, J.P., Charles, D.F., Hughes, R.M., Paulsen, S.G., Collins, G.B., 1999. Assessing water quality changes in the lakes of the northeastern United States using sediment diatoms. *Canadian Journal of Fisheries and Aquatic Sciences* 56, 131–152.

Engstrom, D.R., Wright, H.E., 1984. Chemical stratigraphy of lake sediments as a record of environmental change. In: Haworth, E.Y., Lund, J.G. (Eds.), *Lake Sediments and Environmental History*. Leicester University Press, Leicester, UK, pp. 11–67.

Grosjean, M., Valero-Garcés, B.L., Geyh, M.A., Messerli, B., Schotterer, U., Schreier, H., Kelts, K., 1997. Mid- and late-holocene limnogeology of Laguna del Negro Francisco, northern Chile, and its palaeoclimatic implications. *The Holocene* 7 (2), 151–159.

Hasle, G., Fryxell, G., 1970. Diatoms: cleaning and mounting for light and electron microscopy. *Transactions of American Microscopy Society* 89, 469–474.

Heusser, C.J., 1983. Quaternary pollen record from Laguna de Tagua Tagua, Chile. *Science* 219, 1429–1432.

Heusser, C.J., 1990. Ice age vegetation and climate of subtropical Chile. *Palaeogeography, Palaeoclimatology, Palaeoecology* 80, 107–127.

Keefer, D.K., deFrance, S.D., Moseley, M.E., Richardson III, J.B., Satterlee, D.R., Day-Lewis, A., 1998. Early maritime economy

- and El Niño events at Quebrada Tacahuay, Peru. *Science* 281, 1833–1835.
- Kemp, A.L.W., Thomas, R.L., Dell, C.I., Jaquet, J.M., 1976. Cultural impact on the geochemistry of sediments in Lake Erie. *Journal of the Fisheries Research Board of Canada* 33, 440–462.
- Krammer, K., Lange-Bertalot, H., 1988. *Suesswasserflora von Mitteleuropa. Bacillariophyceae, Teil II: Bacillariophyceae, Epithemiaceae, Surirellaceae*. Gustav Fischer Verlag, Stuttgart, p. 576.
- Krammer, K., Lange-Bertalot, H., 1991a. *Suesswasserflora von Mitteleuropa, Bacillariophyceae, Teil III: Centrales, Fragilariaceae, Eunotiaceae*. Gustav Fischer Verlag, Stuttgart, p. 596.
- Krammer, K., Lange-Bertalot, H., 1991b. *Suesswasserflora von Mitteleuropa, Bacillariophyceae, Teil IV: Achnanthaceae*. Gustav Fischer Verlag, Stuttgart, p. 437.
- Lamy, F., Hebbeln, D., Wefer, G., 1999. High-resolution marine record of climatic change in mid-latitude Chile during the last 28,000 years based on terrigenous sediment parameters. *Quaternary Research* 51, 83–93.
- Lara, A., Villalba, R., 1993. A 3620-year temperature record from *Fitzroya cupressoides* tree rings in southern South America. *Science* 260, 1104–1106.
- Mackereth, F.J.H., 1966. Some chemical observations on post-glacial lake sediments. *Philosophical Transactions of the Royal Society, Series B* 250, 165–213.
- Markgraf, V., 1989. Paleoclimates in central and South America since 18,000 BP based on pollen and lake-level records. *Quaternary Science Reviews* 8, 1–24.
- Markgraf, V., 1998. Past climates of South America. In: Hobbs, J.E., Lindesay, J.A., Bridgman, H.A. (Eds.), *Climates of the Southern Continents. Present, Past and Future*. Wiley, Chichester, 249 pp.
- Mortlock, R.A., Froelich, P., 1989. A simple method for the rapid determination of biogenic opal in pelagic marine sediments. *Deep-Sea Research* 36 (9), 1415–1426.
- Oldfield, F., Appleby, P.G., 1984. Empirical testing of ^{210}Pb dating models. In: Haworth, E.Y., Lund, W.G. (Eds.), *Lake Sediments and Environmental History*. Leicester University Press, Leicester, UK, pp. 93–124.
- Parra, O., Basualto, S., Urrutia, R., Valdovinos, C., 1999. Estudio comparativo de la diversidad fitoplanctónica de cinco lagos de diferentes niveles de eutroficación del área litoral de la Región del Biobío (Chile). *Gayana Botanica* 56 (2), 93–108.
- Quinn, W., Neal, V., Antunez de Mayolo, S., 1987. El Niño occurrences over the past four and a half centuries. *Journal of Geophysical Research* 92 (14), 449–461.
- Rivera, P., 1967. Algunas especies de *Melosira* Agardh en el lago Ranco. *Noticiero Mensual, Museo Nacional de Historia Natural* 135. Santiago, Chile, p. 97.
- Rivera, P., Parra, O., Gonzalez, M., Dellarossa, V., Orellana, M., 1982. *Manual Taxonómico del fitoplancton de aguas continentales*. Editorial Universidad de Concepción, Concepción, p. 97.
- Röthlisberger, F., 1986. *10,000 Jahre Gletschergeschichte der Erde*. Salzburg, Sauerländer, p. 416.
- Sandweiss, D.H., Maasch, K.A., Anderson, D.G., 1999. Transitions in the mid-holocene. *Science* 283, 499–501.
- Schoemann, F., 1973. A systematical and ecological study of the diatom flora of Lesotho with special reference to the water quality. V and R Printers, Pretoria, p. 355.
- Stuiver, M., Reimer, P.J., 1993. Extended ^{14}C database and revised CALIB radiocarbon calibration program. *Radiocarbon* 35, 215–230.
- Stuiver, M., Reimer, P.J., Bard, E., Beck, J.W., Burr, G.S., Hughen, K.A., Kromer, B., McCormac, F.G., Plicht, v.d., Spurk, J., 1998a. INTCAL98 radiocarbon age calibration 24,000–0 cal BP. *Radiocarbon* 40, 1041–1083.
- Stuiver, M., Reimer, P.J., Braziunas, T.F., 1998b. High-precision radiocarbon age calibration for terrestrial and marine samples. *Radiocarbon* 40, 1127–1151.
- Thomasson, K., 1959. Nahuel Huapi. Plankton of some lakes in an Argentine National Park with notes on terrestrial vegetation. *Acta Phytogeographica Suecica* 42, 83.
- Thompson, L.G., Davis, M.E., Mosley-Thompson, E., Sowers, T.A., Henderson, K.A., Zagorodnov, V.S., Lin, P.N., Mikhailenko, V.N., Campen, R.K., Bolzan, J.F., Cole-Dai, J., Francou, B., 1998. A 25,000-year tropical climate history from Bolivian ice cores. *Science* 282, 1858–1864.
- Thompson, L.G., Mosley-Thompson, E., Morales Arnao, B., 1984. El Niño-southern oscillation events recorded in the stratigraphy of the tropical Quelccaya Ice Cap, Peru. *Science* 226, 50–52.
- Valero-Garcés, B.L., Grosjean, M., Schwab, A., Geyh, M.A., Messerli, B., Kelts, K., 1996. Limnogeology of laguna Miscanti: evidence for mid to late Holocene moisture changes in the Atacama Altiplano (Northern Chile). *Journal of Paleolimnology* 16, 1–21.
- Van Dam, H., Mertens, A., Sinkeldam, J., 1994. A coded checklist and ecological indicator values of freshwater diatoms from the Netherlands. *Netherlands Journal of Aquatic Ecology* 28 (1), 117–133.
- Van Husen, C., 1967. Klimagliederung in Chile auf der Basis von Häufigkeitsverteilungen der Niederschlagssummen. *Freiburger Geographische Hefte* 4.
- Veit, H., 1996. Southern Westerlies during the Holocene deduced from geomorphological and pedological studies in the Norte Chico, Northern Chile (27–33°S). *Paleogeography, Palaeoclimatology, Palaeoecology* 123, 107–119.
- Villagrán, C., Varela, J., 1990. Palynological evidence for increased aridity on the central Chilean coast during the Holocene. *Quaternary Research* 34, 198–207.
- Villalba, R., 1994a. Fluctuaciones climáticas en latitudes medias de América del Sur durante los últimos 1000 años: sus relaciones con la Oscilación del Sur. *Revista Chilena de Historia Natural* 67, 453–461.
- Villalba, R., 1994b. Tree-ring and glacial evidence for the medieval warm epoch and the little ice age in southern South America. *Climatic Change* 26 (2), 183–197.
- Villa-Martínez, R., Villagrán, C., 1997. Historia de la vegetación de bosques pantanosos de la costa de Chile central durante el Holoceno medio y tardío. *Revista Chilena de Historia Natural* 70, 391–401.
- Weischet, W., 1996. *Regionale Klimatologie, Teil I: Die neue Welt*. Stuttgart. B.G. Teubner, p. 468.
- Wells, L.E., 1990. Holocene history of the El Niño phenomenon as recorded in flood sediments of northern coastal Peru. *Geology* 18, 1134–1137.
- Wirmann, D., Mourguiart, P., 1995. Late quaternary spatio-temporal limnological variation in the Altiplano of Bolivia and Peru. *Quaternary Research* 43, 344–354.